

AUDIOFUSE: UNIFIED SPECTRAL-TEMPORAL LEARNING VIA A HYBRID VIT-1D CNN ARCHITECTURE FOR ROBUST PHONOCARDIOGRAM CLASSIFICATION

Md. Saiful Bari Siddiqui, Utsab Saha

Department of Computer Science and Engineering, BRAC University, Dhaka, Bangladesh

ABSTRACT

Biomedical audio signals, such as phonocardiograms (PCG), are inherently rhythmic and contain diagnostic information in both their spectral (tonal) and temporal domains. Standard 2D spectrograms provide rich spectral features but compromise the phase information and temporal precision of the 1D waveform. We propose AudioFuse, an architecture that simultaneously learns from both complementary representations to classify PCGs. To mitigate the overfitting risk common in fusion models, we integrate a custom, wide-and-shallow Vision Transformer (ViT) for spectrograms with a shallow 1D CNN for waveforms. On the PhysioNet 2016 dataset, AudioFuse achieves a state-of-the-art competitive ROC-AUC of 0.8608 when trained from scratch, outperforming its spectrogram (0.8066) and waveform (0.8223) baselines. Moreover, it demonstrates superior robustness to domain shift on the challenging PASCAL dataset, maintaining an ROC-AUC of 0.7181 while the spectrogram baseline collapses (0.4873). Fusing complementary representations thus provides a strong inductive bias, enabling the creation of efficient, generalizable classifiers without requiring large-scale pre-training.

Index Terms— Acoustic signal classification, Biomedical signal processing, Convolutional neural networks, Deep learning, Representation learning, Vision transformers.

1. INTRODUCTION

The analysis of biomedical audio signals is a critical and rapidly growing field, offering the potential for low-cost, non-invasive, and scalable diagnostic tools. A significant portion of these signals, such as phonocardiograms (PCG) and respiratory audio, are inherently rhythmic. Their diagnostic value is encoded not just in their spectral content (such as the frequency of a heart murmur), but also in their fine-grained temporal dynamics, including the precise timing, duration, and morphology of acoustic events like S1/S2 heart sounds. The dominant paradigm for biomedical audio classification involves converting the 1D time-series signal into a 2D representation[1], typically a log-Mel spectrogram, and applying powerful vision-based deep learning models like CNNs or Transformers [2, 3, 4, 5]. While this approach

excels at learning complex spectral and harmonic patterns, it creates an inherent trade-off. The windowing function of the Short-Time Fourier Transform (STFT) used to generate spectrograms necessarily blurs temporal details and discards all phase information, potentially obscuring the very transient and rhythmic cues that are diagnostically critical [6], [7]. Conversely, models operating directly on the 1D waveform preserve this temporal precision but struggle to learn the complex frequency relationships that are explicit in a 2D representation [8], [9].

To address this limitation, we propose AudioFuse, a dual-branch architecture designed to simultaneously learn from these complementary spectral and temporal representations. A key challenge with fusion models is the heightened risk of overfitting, due to a potentially large parameter count and increased complexity, especially on the limited-sized biomedical domain datasets [10]. To mitigate this, we specifically design AudioFuse to be lightweight and parameter-efficient. It employs a balanced two-branch design: a custom, wide-and-shallow ViT processes spectrograms to learn global spectral context, while a compact 1D-CNN extracts precise temporal features from the raw waveform. These specialized feature vectors are then integrated via late fusion.

We validate our approach on the challenging task of PCG classification. We use the PhysioNet 2016 dataset to evaluate in-domain performance and the PASCAL dataset to test for out-of-domain generalization. Our experimental results show that AudioFuse, when trained from scratch, significantly outperforms its single-modality baselines. It also demonstrates substantially improved generalization performance. The main contributions of this work are:

- We propose AudioFuse, a lightweight, dual-branch ViT-1D CNN architecture to fuse complementary spectral and temporal information from audio signals.
- We demonstrate that, when trained from scratch, our fusion model achieves state-of-the-art competitive performance on the PhysioNet 2016 dataset with significantly fewer parameters than typical large-scale models.
- We provide a domain generalization analysis, showing that AudioFuse outperforms its single-modality baselines and is more robust to domain shift.

2. THEORETICAL BACKGROUND

This section establishes the theoretical intuition behind our design choices by examining the complementary nature of 1D and 2D audio representations and the architectural specializations required to process them.

2.1. Complementary 1D and 2D Audio Representations

Let a discrete audio signal be represented as a 1D time-series vector $x[n]$, where n is the sample index. This representation preserves all information, including phase and precise temporal location of events.

Conversely, a 2D log-Mel spectrogram, $S(t, f_{mel})$, is a derived representation. It is generated via the Short-Time Fourier Transform (STFT), which maps the signal from the time domain to a joint time-frequency domain:

$$X(t, \omega) = \sum_{n=-\infty}^{\infty} x[n]w[n-t]e^{-j\omega n} \quad (1)$$

where $w[n]$ is a windowing function. The power spectrogram is then $P(t, \omega) = |X(t, \omega)|^2$, which is subsequently mapped to the Mel scale. The fundamental trade-off here is that to achieve high frequency resolution, the window $w[n]$ must be long. This, however, averages the signal over a longer time period, resulting in poor time resolution and blurring the precise onset of transient events like cardiac valve clicks. Conversely, a short window provides good time resolution but poor frequency resolution. This highlights the complementary nature of the two representations:

- **1D Waveform ($x[n]$):** Possesses high temporal resolution and complete phase information. It is ideal for localizing transient events and analyzing rhythm. Its spectral information, however, is only implicit.
- **2D Spectrogram ($S(t, f_{mel})$):** Possesses high spectral resolution, making harmonic structures visually explicit. It is ideal for analyzing tonal components like murmurs or wheezes. Its temporal information is inherently compromised.

No single representation is optimal for all diagnostic features present in a biomedical signal. Therefore, a model that can leverage the strengths of both is theoretically superior. Several approaches ranging from traditional ML [11] to Encoder-Decoder architectures [3] have been explored for heart sound classification by researchers, but very few works have been done to combine these two complementary domains.

2.2. Feature Extraction and Fusion

To effectively learn from these two disparate representations, we require specialized network architectures for each branch.

For the image-like spectrogram, the **ViT**[12] is exceptionally well-suited. Its self-attention mechanism[13] allows it to learn global, long-range dependencies across the entire time-frequency plane, enabling it to model the overall structure and evolution of harmonic patterns more effectively than the local receptive fields of a traditional CNN.

For the sequential waveform, a **1D-CNN** is an ideal choice. Its 1D kernels act as learnable matched filters that slide along the time axis, making them highly efficient at detecting specific, short-duration temporal patterns and wave morphologies that characterize transient events. Given that the two representations contain fundamentally different and complementary types of information, it is crucial to allow each specialized network to extract a high-level feature representation independently, without premature mixing. Therefore, we adopt a **late-fusion** strategy [14]. The ViT and 1D-CNN branches act as independent feature extractors, each processing its preferred modality. The final, high-level feature vectors from each branch are then fused. This allows a subsequent classification head to learn the final, complex decision boundary based on the summarized, high-level insights from both the spectral and temporal domains, preserving the integrity of each feature extraction process.

3. PROPOSED METHOD: AUDIOFUSE

We propose **AudioFuse**, a lightweight, two-branch architecture that robustly classifies biomedical audio by fusing its complementary spectral and temporal representations. The dual-domain model is shown in Fig. 1.

3.1. Spectrogram Branch

The spectral branch is designed to learn global context from the harmonic and tonal structures within a 2D log-Mel spectrogram. For this task, we designed a custom wide-and-shallow Vision Transformer (ViT). The input 224×224 spectrogram is first transformed into a sequence of 196 patch embeddings, each with a dimensionality of 192, via a `Conv2D` layer with a 16×16 kernel. After learnable positional embeddings are added, this sequence is processed by a stack of 6 Transformer encoder blocks. Each block employs a Multi-Head Self-Attention layer with 8 heads and a feed-forward MLP. The final output sequence is then globally averaged to produce a single 192-dimensional spectral feature vector, \mathbf{f}_{spec} . This shallow design captures essential global patterns while minimizing the parameter depth to prevent overfitting.

3.2. Waveform Branch

The temporal branch is designed to learn precise, timing-based features directly from the raw 1D audio waveform, which is padded or truncated to a fixed length of 5 seconds (110,250 samples). We employ a compact 1D Convolutional

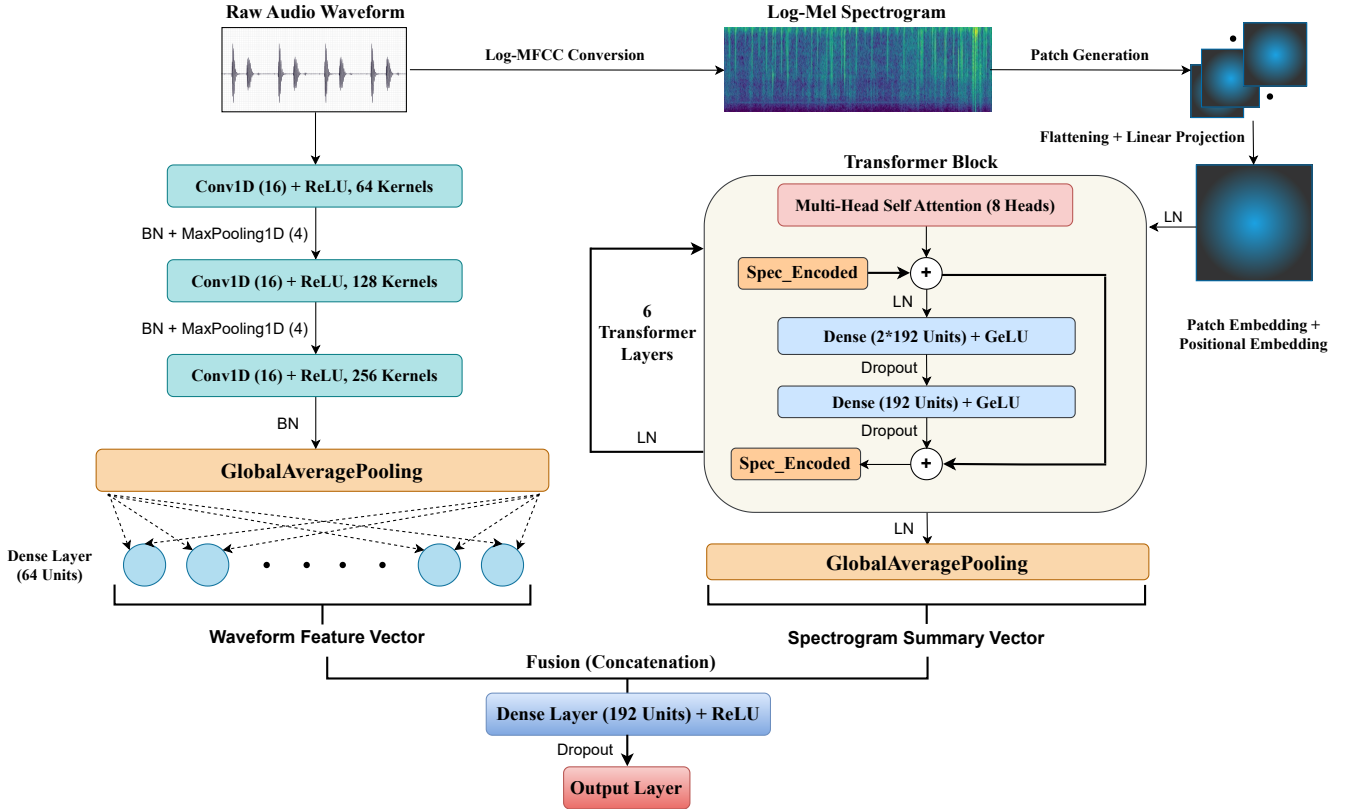


Fig. 1. The AudioFuse architecture. The 2D spectrogram and 1D waveform are processed by parallel ViT and 1D-CNN branches, respectively. The resulting feature vectors are concatenated and passed to a final MLP for classification.

Neural Network (CNN) for this task. The network consists of three sequential Conv1D blocks with increasing filter sizes (64, 128, 256) and a kernel size of 16. Each block uses a stride of 4 and is followed by Batch Normalization and Max-Pooling, allowing the model to learn hierarchical temporal patterns at multiple resolutions. After the final block, the feature sequence is globally averaged and passed through a final Dense layer with 64 units, to produce a compact 64-dimensional temporal feature vector, \mathbf{f}_{wave} .

3.3. Late Fusion Head

The two specialized feature vectors are integrated for the final classification employing late fusion. The spectral feature vector (\mathbf{f}_{spec}) and the temporal feature vector (\mathbf{f}_{wave}) are concatenated to form a single 256-dimensional fused vector:

$$\mathbf{f}_{fused} = [\mathbf{f}_{spec}; \mathbf{f}_{wave}] \quad (2)$$

This vector is then passed through a simple MLP head, which consists of a single Dense layer with 192 units, a high-rate (0.5) Dropout layer for regularization, and a final sigmoid output layer. This design allows the model to learn a final decision boundary based on the high-level, complementary insights from both the spectrogram and temporal branches.

4. RESULTS AND DISCUSSION

4.1. Datasets

We utilize two public phonocardiogram (PCG) datasets. For in-domain training and evaluation, we use the **PhysioNet 2016 Challenge Dataset** [15], [16]. The official split of PhysioNet is known to contain recordings from patients who are also present in the training set, creating a risk of data leakage. To ensure a scientifically valid evaluation, we identified and removed all such instances from our training data. For out-of-domain generalization testing, we use the **PASCAL Classifying Heart Sounds Dataset** [17]. Specifically, we use the small, more challenging **Set B**, whose recordings were crowdsourced via the iStethoscope application, resulting in a significant domain shift from the cleaner, clinical-grade PhysioNet data. The train-test split was done based on the Patient IDs.

4.2. Implementation Details and Compared Models

All models were trained for up to 200 epochs using the AdamW optimizer (learning rate 3×10^{-4} , weight decay 1×10^{-4}). Data imbalance was addressed through manual class weighting. We employed early stopping with a patience

Table 1. Model Performance Comparison on PhysioNet 2016. All models were trained from scratch. Results are reported as Mean \pm Standard Deviation over multiple independent runs. The best result for each metric is highlighted in **bold**.

Model	# Params	Accuracy	F1-Score	ROC-AUC	MCC
Spectrogram Baseline (ViT)	1.83M	0.7193 ± 0.0071	0.7383 ± 0.0197	0.8066 ± 0.0141	0.4444 ± 0.0211
Raw Audio Baseline (1D-CNN)	675K	0.7376 ± 0.0094	0.7057 ± 0.0260	0.8223 ± 0.0313	0.4884 ± 0.0085
Spectrogram-Scalogram Fusion	1.96M	0.6611 ± 0.0215	0.6107 ± 0.0280	0.7478 ± 0.0251	0.3349 ± 0.0312
AudioFuse (Cross-Attention)	2.69M	0.7276 ± 0.0152	0.7485 ± 0.0189	0.8226 ± 0.0161	0.4608 ± 0.0240
AudioFuse (Gated FiLM)	2.57M	0.7575 ± 0.0110	0.7622 ± 0.0152	0.8518 ± 0.0141	0.5152 ± 0.0186
AudioFuse (Concatenation)	2.56M	0.7741 ± 0.0094	0.7664 ± 0.0005	0.8608 ± 0.0127	0.5508 ± 0.0225
MobileNetV3 [18]	5.4M	0.6677 ± 0.0165	0.6627 ± 0.0218	0.7509 ± 0.0204	0.3454 ± 0.0239
EfficientNetB0 [19]	5.3M	0.6467 ± 0.0041	0.6349 ± 0.0093	0.7472 ± 0.0177	0.4792 ± 0.0113
ResNet18 [20]	11.7M	0.7375 ± 0.0071	0.7365 ± 0.0080	0.8336 ± 0.0068	0.4792 ± 0.0113
DenseNet169 [21]	14.3M	0.7464 ± 0.0284	0.7442 ± 0.0287	0.8640 ± 0.0181	0.5023 ± 0.0578
InceptionV3 [22]	23.8M	0.7621 ± 0.0181	0.7572 ± 0.0212	0.8581 ± 0.0089	0.5356 ± 0.0005

of 30 epochs on validation accuracy.

We compare our proposed AudioFuse (concatenation fusion) against two single-modality baselines (a Spectrogram ViT and a Waveform 1D-CNN) whose architectures are identical to the branches of our fusion model. We also provide an ablation study on alternative fusion strategies, Gated (FiLM), Cross-Attention mechanisms, and also a Spectrogram-Scalogram fusion.

4.3. Performance on PhysioNet 2016

The primary performance of all models was evaluated on the curated PhysioNet 2016 validation set. Table 1 summarizes these results. Our proposed AudioFuse model with concatenation fusion emerges as the top-performing architecture across all key metrics.

The single-modality baselines demonstrate competent but limited performance. The Raw Audio Baseline (ROC-AUC 0.8223) slightly outperforms the Spectrogram Baseline (0.8066), underscoring the importance of the temporal information preserved in the 1D waveform. The Spectrogram-Scalogram fusion performs poorly, indicating overfitting and that its input modalities are largely redundant.

While the more complex Gated FiLM and Cross-Attention fusion strategies show improvements over the baselines, they do not surpass the simple yet effective late-fusion concatenation. This suggests that for this task, a robust concatenation of specialized features is more stable and easier to optimize than more intricate fusion mechanisms. AudioFuse achieves an ROC-AUC of 0.8608 ± 0.0127 , a significant improvement over the best-performing baselines.

Most importantly, despite being trained from scratch and having only 2.56M parameters, AudioFuse outperforms all the SOTA architectures trained on spectrograms in overall Accuracy, F1-Score, and Matthews Correlation Coefficient. Only DenseNet169 marginally beats AudioFuse in terms of ROC-AUC, but our model remains highly competitive with nearly 6 times fewer parameters.

Standard architectures, regardless of their depth or complexity, are fundamentally limited to the information present in a single view of the data, the spectrogram. AudioFuse circumvents this limitation. Its ViT branch is free to specialize in learning the global spectral patterns of the spectrogram, while the 1D-CNN branch independently captures the precise, high-resolution temporal dynamics from the raw waveform. The model is fed a richer, more disentangled set of features from the very same audio signal. It can simply learn more with less complexity. These results show that for rhythmic biomedical audio, our dual-representation fusion architecture can achieve better performance than a deeper, larger, single-input model, even with a lightweight design.

4.4. Domain Generalization Performance on PASCAL

A crucial test of a model’s utility is its ability to generalize to unseen data from different recording environments. We evaluated our three strongest models on the PASCAL dataset in a zero-shot context, using the weights trained solely on PhysioNet and fine-tuning the final dense layers. The results, shown in Table 2, highlight the superior robustness of our fusion approach.

Table 2. Model Performance on the PASCAL Dataset

Model	Acc.	F1-Score	ROC-AUC	MCC
ViT	0.5795	0.3273	0.4873	0.0579
1D CNN	0.6818	0.5484	0.6782	0.3152
AudioFuse	0.7386	0.6667	0.7181	0.4519

The Spectrogram Baseline’s performance collapses entirely, with an ROC-AUC of 0.4873 indicating performance worse than random chance. This suggests it overfitted to the specific acoustic characteristics of the PhysioNet data. The Raw Audio Baseline proves significantly more robust, maintaining a reasonable ROC-AUC of 0.6782, demonstrating that temporal features are less susceptible to this domain shift.

Once again, AudioFuse Concatenation achieves the best performance, with an ROC-AUC of 0.7181. This result is a dramatic improvement over both baselines. It demonstrates that by learning from two complementary representations, our model develops a more holistic and resilient understanding of the underlying cardiac sounds, making it far more generalizable and better suited for real-world applications where data variability is expected.

5. CONCLUSION

In this work, we proposed AudioFuse, a lightweight, hybrid ViT-1D CNN architecture for robust biomedical audio classification. Our experiments demonstrated that by simultaneously learning from complementary spectral (spectrogram) and temporal (waveform) representations, our model, trained from scratch, achieves state-of-the-art competitive performance on the PhysioNet 2016 dataset. Moreover, it shows vastly superior robustness to domain shift on the challenging PASCAL dataset compared to its single-modality baselines.

Our results underline the importance of utilizing multiple complementary representations of signals. It also indicates that a carefully designed fusion architecture provides a powerful inductive bias for rhythmic biomedical signals, enabling the creation of powerful, parameter-efficient, and generalizable classifiers without the need for large-scale pre-training. This paradigm opens several promising directions for future work. The AudioFuse concept can be directly extended to other challenging biomedical audio tasks where both tonal and transient features are critical, such as detecting crackles and wheezes in respiratory audio or analyzing cough sounds. Exploring more advanced attention-based fusion mechanisms and optimizing the architecture for on-device deployment could pave the way for its use in real-time, mobile health monitoring applications. Furthermore, future work could explore scaling up these specialized branch architectures to leverage large-scale audio datasets, potentially rivaling the performance of heavily pre-trained models while retaining the benefits of a multi-representation learning approach.

6. DATA AND CODE AVAILABILITY

Both the datasets we used for this study are publicly available. The complete source code and pretrained model weights for our baseline and AudioFuse models are publicly available on GitHub at: [https://github.com/Saiful185/](https://github.com/Saiful185/AudioFuse) AudioFuse.

7. REFERENCES

- [1] Y. Gong, Y.-A. Chung, and J. Glass, “AST: Audio spectrogram transformer,” in *Proc. Interspeech*, 2021.
- [2] Z. Liu, W. Liu, Z. Gu, and F. Yang, “Efficient anomaly detection algorithm for heart sound signal,” *IEEE Access*, 2024.
- [3] R. Banerjee and A. Ghose, “A semi-supervised approach for identifying abnormal heart sounds using variational autoencoder,” in *ICASSP 2020-2020 IEEE International Conference on Acoustics, Speech and Signal Processing (ICASSP)*. IEEE, 2020, pp. 1249–1253.
- [4] W. Zhao, H. Ma, N. Jin, Y. Zheng, and X. Guo, “Detection of coronary heart disease based on heart sound and hybrid vision transformer,” *Applied Acoustics*, vol. 230, pp. 110420, 2025.
- [5] A. Sharma et al., “Spectronet-lstm: An interpretable deep learning approach to cardiac anomaly detection through heartbeat sound analysis,” *Computers in Biology and Medicine*, vol. 196, pp. 110774, 2025.
- [6] N. B. Thien, Y. Wakabayashi, Y. Geng, K. Iwai, and T. Nishiura, “Weighted von mises distribution-based loss function for real-time STFT phase reconstruction using DNN,” in *Proc. Interspeech*, 2023, pp. 3864–3868.
- [7] D. Griffin and J. Lim, “Signal estimation from modified short-time fourier transform,” *IEEE Transactions on Acoustics, Speech, and Signal Processing*, vol. 32, no. 2, pp. 236–243, 1984.
- [8] A. Natsiou and S. O’Leary, “Audio representations for deep learning in sound synthesis: A review,” in *Proc. IEEE/ACS 18th Int. Conf. Computer Systems and Applications (AICCSA)*, 2021, pp. 1–8.
- [9] G. Peeters and G. Richard, “Deep learning for audio and music,” in *Multi-faceted Deep Learning*, J. Benois-Pineau and A. Zemmari, Eds., pp. 231–266. Springer, Cham, 2021.
- [10] V. Guerrasi, F. Aksu, C. M. Caruso, F. Di Feola, A. Rofena, F. Ruffini, and P. Soda, “A systematic review of intermediate fusion in multimodal deep learning for biomedical applications,” *Image and Vision Computing*, vol. 158, 2025.
- [11] Y. Zeinali and S. T. A. Niaki, “Heart sound classification using signal processing and machine learning algorithms,” *Biomedical Signal Processing and Control*, vol. 68, 2021.

- [12] A. Dosovitskiy, L. Beyer, A. Kolesnikov, D. Weissenborn, X. Zhai, T. Unterthiner, M. Dehghani, M. Minderer, G. Heigold, S. Gelly, J. Uszkoreit, and N. Houlsby, “An image is worth 16x16 words: Transformers for image recognition at scale,” in *Proc. Int. Conf. Learn. Representations (ICLR)*, 2021.
- [13] A. Vaswani, N. Shazeer, N. Parmar, J. Uszkoreit, L. Jones, A. N. Gomez, L. Kaiser, and I. Polosukhin, “Attention is all you need,” in *Advances in Neural Information Processing Systems (NeurIPS)*, 2017, pp. 5998–6008.
- [14] J. Ngiam, A. Khosla, M. Kim, J. Nam, H. Lee, and A. Y. Ng, “Multimodal deep learning,” in *Proceedings of the 28th International Conference on International Conference on Machine Learning*, Madison, WI, USA, 2011, ICML’11, p. 689–696, Omnipress.
- [15] C. Liu et al., “An open access database for the evaluation of heart sound algorithms,” *Physiological Measurement*, vol. 37, no. 12, pp. 2181, Nov. 2016.
- [16] A. L. Goldberger et al., “Physiobank, physiotoolkit, and physionet: Components of a new research resource for complex physiologic signals,” *Circulation*, vol. 101, no. 23, pp. e215–e220, 2000.
- [17] P. Bentley, G. Nordehn, M. Coimbra, S. Mannor, and R. Getz, “The PASCAL classifying heart sounds challenge 2011 (CHSC2011) results,” in *Proc. Computing in Cardiology (CinC)*, 2011, pp. 1–4.
- [18] A. Howard, M. Sandler, G. Chu, L.-C. Chen, B. Chen, M. Tan, W. Wang, Y. Zhu, R. Pang, V. Vasudevan, Q. V. Le, and H. Adam, “Searching for MobileNetV3,” in *Proc. IEEE/CVF Int. Conf. Computer Vision (ICCV)*, 2019, pp. 1314–1324.
- [19] M. Tan and Q. V. Le, “Efficientnet: Rethinking model scaling for convolutional neural networks,” in *Proc. Int. Conf. Machine Learning (ICML)*. 2019, pp. 6105–6114, PMLR.
- [20] K. He, X. Zhang, S. Ren, and J. Sun, “Deep residual learning for image recognition,” in *Proc. IEEE Conf. Computer Vision and Pattern Recognition (CVPR)*, 2016, pp. 770–778.
- [21] G. Huang, Z. Liu, L. Van Der Maaten, and K. Q. Weinberger, “Densely connected convolutional networks,” in *Proc. IEEE Conf. Computer Vision and Pattern Recognition (CVPR)*, 2017, pp. 2261–2269.
- [22] C. Szegedy, V. Vanhoucke, S. Ioffe, J. Shlens, and Z. Wojna, “Rethinking the inception architecture for computer vision,” in *Proc. IEEE Conf. Computer Vision and Pattern Recognition (CVPR)*, 2016, pp. 2818–2826.